

# Experimental and DFT Studies on the Behavior of Caffeine as Effective Corrosion Inhibitor of Copper in 1M HNO<sub>3</sub>

Victorien Kouakou, Paulin M. Niamien\*, Aboua J. Yapo, Sékou Diaby, Albert Trokourey

*Laboratoire de Chimie Physique de l'Université Félix Houphouët Boigny, Abidjan-Cocody, Ivory Coast.*

Article history: Received: 23 October 2015; revised: 08 January 2016; accepted: 09 January 2016. Available online: 31 March 2016. DOI: <http://dx.doi.org/10.17807/orbital.v8i2.804>

**Abstract:** Caffeine was tested as copper corrosion inhibitor in 1M HNO<sub>3</sub> using mass loss technique at 308-328K and theoretical studies based on quantum chemistry. The inhibition efficiency is concentration and temperature dependent: Caffeine showed an inhibition efficiency of 78% at 5mM for T =328K. The thermodynamic adsorption parameters ( $\Delta G_{ads}^0$ ,  $\Delta H_{ads}^0$ ,  $\Delta S_{ads}^0$ ) were determined and analyzed. They revealed a spontaneous adsorption process and a strong interaction between Caffeine and the metal surface. Adsorption isotherms including Langmuir, Temkin and El-Awady were tested. It was found that Caffeine adsorbs on copper according to the modified Langmuir adsorption isotherm. The Dubinin Raduskevitch model was used to distinguish between chemisorption and physisorption. Activation parameters ( $E_a$ ,  $\Delta H_a^*$ ,  $\Delta S_a^*$ ) were also determined and discussed. Furthermore, the quantum chemical properties/descriptors most relevant to the potential action of the molecule as corrosion inhibitor such as highest occupied molecular energy ( $E_{HOMO}$ ), lowest unoccupied molecular orbital energy ( $E_{LUMO}$ ), energy gap( $\Delta E$ ), dipole moment ( $\mu$ ) and charges on heteroatoms were calculated using DFT at B3LYP level with 6-31+G (d) and LanL2DZ basis sets. Fukui indices were also determined and discussed. The theoretical results are consistent with the experimental data reported.

**Keywords:** nitric acid; caffeine; mass loss; corrosion inhibition; adsorption isotherm; quantum parameters

## 1. INTRODUCTION

Studies on corrosion and corrosion inhibition of metals in acidic media, particularly copper corrosion and its inhibition in nitric acid [1] is of interest in many industries. Indeed, copper [2, 3] is a widely used metal due to its excellent corrosion resistance, mechanical, thermal and electrical conductivity properties. On the other hand, nitric acid solution [4] is the corrosive solution of choice in many processes used in fabrication (electroplating, chemical dissolution, etc.). Unfortunately, copper [5] undergoes corrosion when it is in contact with nitric acid solution what causes a loss of its mechanical properties. Thus, much attention [6-8] has been focused on the behavior of various inhibitors to find chemical compounds for preventing copper corrosion. The use of organic chemical inhibitors is one of the most practical methods for the protection against corrosion in acidic media. Most of the excellent acid inhibitors are heterocyclic organic compounds containing nitrogen [9-11], oxygen [12-15], phosphorous [16] and sulphur [17-20]. However, a very important disadvantage of these heterocyclic

compounds is their toxicity [21] and most of them cannot be biodegradable. This lack of biodegradability leads to the emission of industrial waste water carrying a large amount of toxic material to public water ways. A possible solution to this problem is to find new ecologically, friendly corrosion inhibitors. Natural products [22-24] extracted from plant sources, as well as some nontoxic organic compounds [25, 26] which contain polar functions with nitrogen, oxygen, sulphur and/or phosphorous in their molecules have been effectively used as inhibitors in many corrosion systems.

Quantum chemical calculations have been widely used to study reactions mechanisms. They have proved [27-29] to be a very important tool for studying corrosion inhibition mechanisms. Actually, Density Functional Theory (DFT) has become an attractive theoretical method because it gives exact basic vital parameters for even huge complex molecules at low cost. Moreover, sophisticated computational tools, can allow understanding reactivity behavior using hard and soft acid-base (HSAB) theory [30] that provides a

\*Corresponding author. E-mail: [niamienfr@yahoo.fr](mailto:niamienfr@yahoo.fr)

systematic way for the analysis of the inhibitor/surface interaction. Thus, DFT has become the main source of connecting some traditional empirical concepts with quantum mechanics. Therefore, DFT is a very powerful technique to probe the inhibitor/surface interaction and to analyze experimental data.

The aim of this work is to highlight the relationship between the calculated quantum chemical parameters and the experimentally determined inhibition efficiency of caffeine against copper corrosion in 1M HNO<sub>3</sub>. This can be achieved by calculating the most relevant molecular properties of the molecule, including  $E_{HOMO}$ ,  $E_{LUMO}$ , energy gap ( $\Delta E$ ), dipole moment ( $\mu$ ), electronegativity ( $\chi$ ), global hardness ( $\eta$ ), fraction of electrons transferred ( $\Delta N$ ) and charges ( $\delta$ ) on atoms.

## 2. MATERIAL AND METHODS

### 2.1 Copper specimens

The copper specimens were in form of rod measuring 10 mm in length and 2.2 mm of diameter. They were cut in commercial copper of purity 95%.

### 2.2 The studied molecule

affeine (formula:  $C_8H_{10}N_4O_2$ ) structure is given by Figure 1.

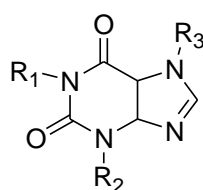


**Figure 1.** Chemical structure of Caffeine ( $R_1 = R_2 = R_3 = CH_3$ )

### 2.3 Solutions

Analytical grade 65% nitric acid solution from Merck was used to prepare the corrosive aqueous solution. The solution was prepared by dilution of the commercial nitric acid solution using double distilled water. The blank was a 1M HNO<sub>3</sub> solution. Caffeine of analytical grade was acquired from Sigma Aldrich chemicals and solutions of concentrations range from 0.1 to 5mM were prepared.

### 2.4 Mass loss measurements

The mass loss measurements were carried out in a 100 mL capacity glass baker placed in a thermostat water bath. The solution volume was 50 mL. The samples were weighed and immersed in 50 mL of an aerated 1.0 M HNO<sub>3</sub> solution without or with the desired concentration of caffeine for 1h exposure period of time at a given temperature (precision:  $\pm 0.5^\circ\text{C}$ ). At the end of the tests, the samples were taken out, washed again with double distilled water, dried and reweighed using an analytical balance (precision:  $\pm 0.1$  mg). Triplicate measurements were performed in each case and the mean value of the mass loss has been reported. The standard deviation of the observed mass loss was  $\pm 1\%$ . The corrosion rate  $W$  (expressed in  $\text{mg}\cdot\text{cm}^{-2}\cdot\text{h}^{-1}$ ) as well as the inhibition efficiency  $IE$  (%) were calculated using the following equations:

$$W = \frac{\Delta m}{S t} \quad (1)$$

$$IE(\%) = \frac{W - W_{inh}}{W} * 100 \quad (2)$$

Where  $\Delta m$  is the mass loss,  $S$  is the total surface of the sample,  $t$  is the immersion time,  $W$  and  $W_{inh}$  are respectively the corrosion rate without and with a given concentration of caffeine.

### 2.5 Quantum chemistry calculations

Complete geometrical optimization of the investigated molecule has been performed using DFT (Density Functional Theory) with the Becke's three parameters exchange functional along with the Yang-Parr non local correlation functional B3LYP [31-33] with respectively 6-31+G(d) and LanL2DZ basis sets implemented in Gaussian 03 W package [34]. Quantum chemical descriptors including the LUMO energy ( $E_{LUMO}$ ), the HOMO energy ( $E_{HOMO}$ ), the HOMO-LUMO energy gap ( $\Delta E$ ), the dipole moment ( $\mu$ ) and Mulliken atomic charges ( $\delta$ ) were calculated. Furthermore, the reactivity parameters such as ionization energy ( $I$ ), electronic affinity ( $A$ ), electronegativity ( $\chi$ ), global hardness ( $\eta$ ), global softness ( $S$ ) and the fraction of electrons transferred ( $\Delta N$ ) were derived from the quantum chemical descriptors. Fukui indices were determined and analyzed.

## 3. RESULTS AND DISCUSSION

### 3.1 Effect of concentration and temperature on corrosion rate

The variations of corrosion rate with temperature and concentration are presented in Figure 2.

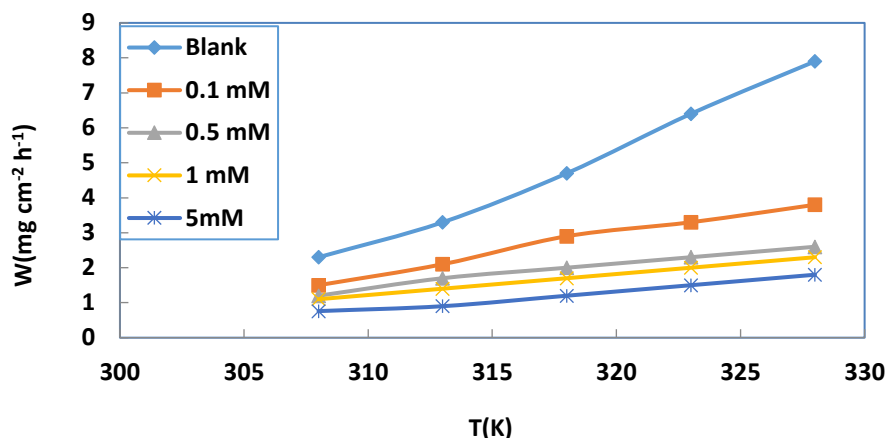


**Figure 2.** Corrosion rate versus temperature for different concentrations.

From Figure 2, one can deduce that corrosion rate increases with increasing temperature for all concentrations. For a given temperature, it is clear that corrosion rate decreases drastically with increasing

concentration of caffeine. Figure 3 presents the evolution of inhibition efficiency with temperature for different concentrations.

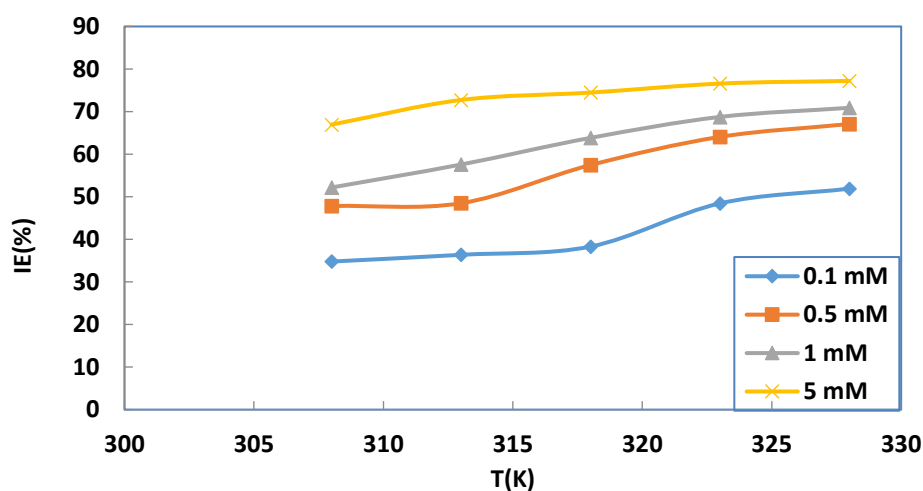


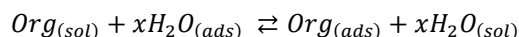
**Figure 3.** Inhibition efficiency versus temperature for different concentrations.

Inhibition efficiency increases with increasing temperature for all the range of concentrations. For a given temperature, inhibition efficiency increases when the concentration increases. All these observations show that Caffeine acts as an effective inhibitor of copper corrosion over the concentration range studied. This behavior could be explained by the formation of a barrier which separates copper from the nitric acid solution.

### 3.2 Adsorption isotherms and thermodynamic parameters

The adsorption of caffeine on the surface of copper can be well interpreted by finding a suitable isotherm which describes the variation of experimentally obtained values of the amount of adsorbate by unit area of the metal surface with its concentration in bulk solution at constant temperature. The adsorption of adsorbate on the metal surface [35]

is regarded as a substitutional adsorption process between the organic compound in the aqueous phase and water molecule adsorbed on the metal surface:



Where,  $Org_{(sol)}$  and  $Org_{(ads)}$  are respectively the adsorbates in the bulk solution and adsorbed on the surface;  $H_2O_{(ads)}$  and  $H_2O_{(sol)}$  are water molecules adsorbed on the surface and in the solution. The number of water molecules replaced by one organic molecule is expressed by  $x$  (the size ratio). Attempts were made to fit values of the degree of surface coverage ( $\theta$ ) which represents the part of metal surface covered by the adsorbate to three isotherms including, Langmuir, Temkin and El-Awady. The equations of these isotherms are given in table 1.

In Table 1,  $C_{inh}$  is Caffeine concentration,  $K_{ads}$  is the equilibrium constant of the adsorption process,  $f$  is a factor of energetic inhomogeneity in the surface,  $\theta$  is the coverage rate while  $K$  is related to  $K_{ads}$  ( $K_{ads} = K^{1/y}$ ).  $1/y$  lower than one suggests multilayer adsorption; in the contrary case  $1/y$  represents the

number of surface sites occupied by one molecule of adsorbate.

**Table 1.** Equations of the tested adsorption isotherms.

Isotherm	Equation
Langmuir	$\frac{C_{inh}}{\theta} = \frac{1}{K_{ads}} + C_{inh}$
Temkin	$\theta = \frac{2.303}{f} [\log K_{ads} + \log C_{inh}]$
El-Awady	$\log \left( \frac{\theta}{1-\theta} \right) = \log K + y \log C_{inh}$

Figures 4 (A, B and C) give the representations of the tested adsorption isotherms.

The parameters of all the tested isotherms are listed in Table 2.

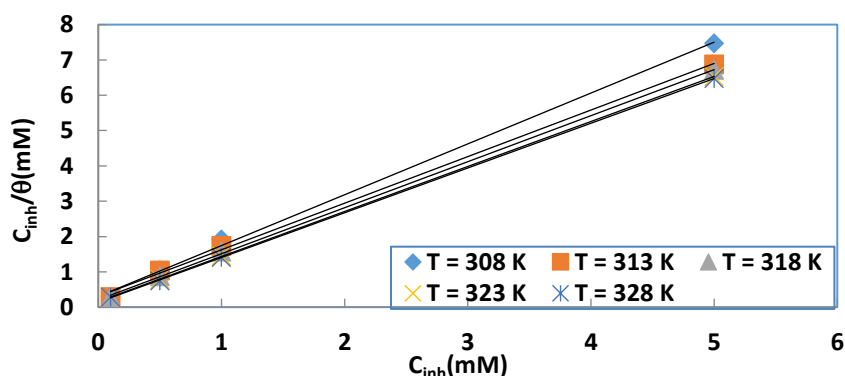


**Figure 4 A.** Langmuir adsorption isotherms for different temperatures.

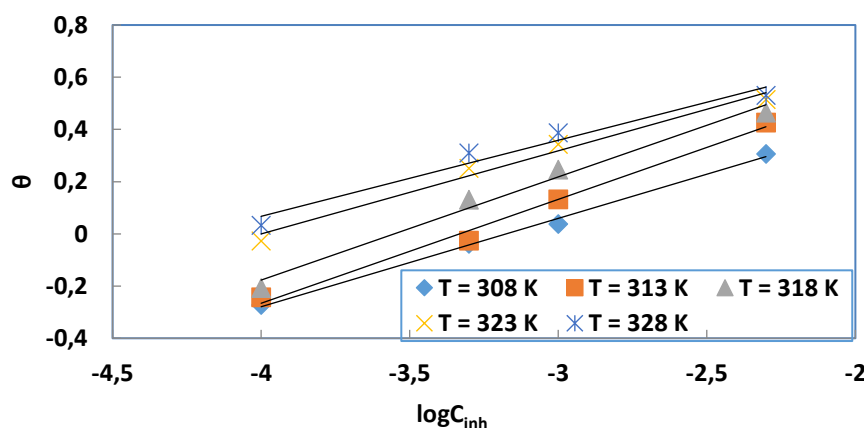


**Figure 4 B.** Temkin adsorption isotherms for different temperatures.

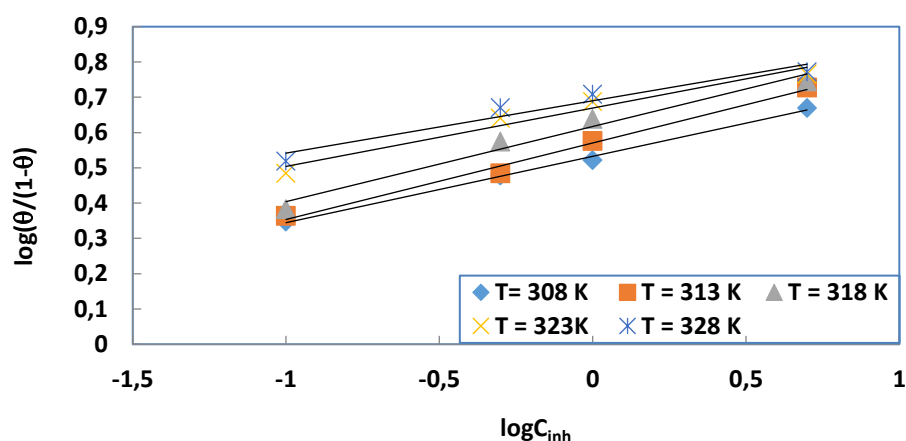


Figure 4 C. El-Awady adsorption isotherms for different temperatures.

Table 2. Isotherms parameters for various temperatures.

Isotherm	T (K)	R <sup>2</sup>	Slope	Intercept
Langmuir	308	0.998	1.4395	0.3040
	313	0.998	1.3200	0.3014
	318	0.999	1.3050	0.1987
	323	0.999	1.2823	0.1268
	328	0.999	1.2766	0.0997
Temkin	308	0.997	0.1880	0.5326
	313	0.992	0.2167	0.5705
	318	0.974	0.2129	0.6172
	323	0.964	0.1653	0.6695
	328	0.943	0.1483	0.6900
El-Awady	308	0.996	0.3384	1.0745
	313	0.991	0.3979	1.3259
	318	0.985	0.3953	1.4040
	323	0.982	0.3183	1.2732
	328	0.966	0.2914	1.2327

The choice of the best adsorption isotherm was based on the values of the correlation coefficients ( $R^2$ ). As it can be seen in table 2, by far Langmuir isotherm is the best adsorption isotherm. However, the deviation

of the slope from unity can be attributable to the molecular interactions among the adsorbed inhibitor species, a factor which was not taken into consideration during the derivation of Langmuir adsorption isotherm

which assumes that:

- The metal surface contains a fixed number of adsorption sites and each site hold one adsorbate.
- The adsorption free energy is the same for all sites and is independent of coverage rate ( $\theta$ ).
- The adsorbates [36] do not interact with one another, i.e. there is no effect of lateral interaction of the adsorbates on the adsorption free energy.

Though the linearity of the Langmuir plot may be interpreted to suggest that the experimental data for Caffeine obey the Langmuir adsorption isotherm, the deviation of the slope from unity showed that the isotherm cannot be strictly applied. The adsorption

behavior of Caffeine can be more appropriately [36] represented by the modified Langmuir equation:

$$\frac{c_{inh}}{\theta} = \frac{n}{K_{ads}} + nC_{inh} \quad (3)$$

Where  $n$  is the slope of the straight line corresponding to the Langmuir isotherm (see  $n$  values in Table 2). The change in standard free energy of adsorption ( $\Delta G_{ads}^0$ ) [37] is related to the adsorption constant ( $K_{ads}$ ) by the following equation:

$$\Delta G_{ads}^0 = -RT \ln(55.5 K_{ads}) \quad (4)$$

The value 55.5 is the concentration of water in solution [38] expressed in mol L<sup>-1</sup>.  $T$  is the absolute temperature while  $R$  is the perfect gas constant. The values of  $K_{ads}$ ,  $\Delta G_{ads}^0$ , are summarized in table 3.

**Table 3.** Thermodynamic parameters of the adsorption of caffeine on copper in 1M HNO<sub>3</sub>.

T(K)	K <sub>ads</sub> (x 10 <sup>3</sup> M <sup>-1</sup> )	$\Delta G_{ads}^0$ (kJ mol <sup>-1</sup> )	$\Delta H_{ads}^0$ (kJ mol <sup>-1</sup> )	$\Delta S_{ads}^0$ (J mol <sup>-1</sup> K <sup>-1</sup> )
308	4.420	-31.75	49.67	262.4
313	3.554	-31.70		
318	5.991	-33.58		
323	9.200	-35.30		
328	11.934	-36.51		

The change in standard adsorption enthalpy  $\Delta H_{ads}^0$  and the change in standard adsorption entropy  $\Delta S_{ads}^0$  are calculated using the following equation:

$$\Delta G_{ads}^0 = \Delta H_{ads}^0 - T \Delta S_{ads}^0 \quad (5)$$

Figure 5 presents the plot of  $\Delta G_{ads}^0$  in function of the temperature. Values of  $\Delta H_{ads}^0$  and  $\Delta S_{ads}^0$  are recorded in table 3. Literature [39, 40] suggests that the values of  $\Delta G_{ads}^0$  of -40 kJ mol<sup>-1</sup> or more negative are associated with chemisorption while the values of -20 kJ mol<sup>-1</sup> or less negative indicate physisorption.

In our case the values of  $\Delta G_{ads}^0$  are within the range of -36.51 kJ mol<sup>-1</sup> to -31.70 kJ mol<sup>-1</sup> indicating a predominant chemisorption process. The negative values of  $\Delta G_{ads}^0$  [41] indicate the stability of the adsorbed layer on the metal surface and the spontaneity of the adsorption process while positive values symbolize a non spontaneous adsorption process. The positive sign of  $\Delta H_{ads}^0$  reflects the endothermic nature

of the adsorption of caffeine on copper in the nitric acid solution. For  $\Delta S_{ads}^0$ , its positive sign indicates that disorder increases when caffeine adsorbs on copper surface due to the desorption of water molecules.

To distinguish between physisorption and chemisorption, experimental data were fitted to Dubinin- Radushkevich isotherm. This model [42, 43] was first used to distinguish between physical adsorption and chemical one for removal of pollutants from aqueous solutions by adsorption on different adsorbents. The model [44] has been recently used to explain the mechanism of corrosion inhibition onto a metal surface in acidic solution. The model is based on the following equation:

$$\ln \theta = \ln \theta_{max} - a \delta^2 \quad (6)$$

Where  $\theta_{max}$  is the maximum surface coverage and  $\delta$  is the Polanyi potential which is given by:

$$\delta = RT \ln \left( 1 + \frac{1}{C_{inh}} \right) \quad (7)$$

In this relation  $R$  is the universal gas constant,  $T$  is the thermodynamic temperature and  $C_{inh}$  is the concentration of the inhibitor. Figure 6 gives the

representation of  $\ln \theta$  in function of  $\delta^2$ .

Table 4 summarizes the parameters of the model.

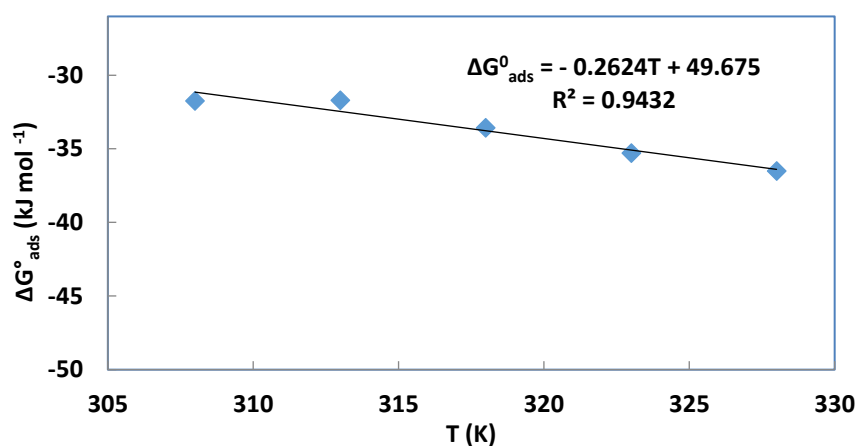


Figure 5. Change in standard Free energy in function of temperature.

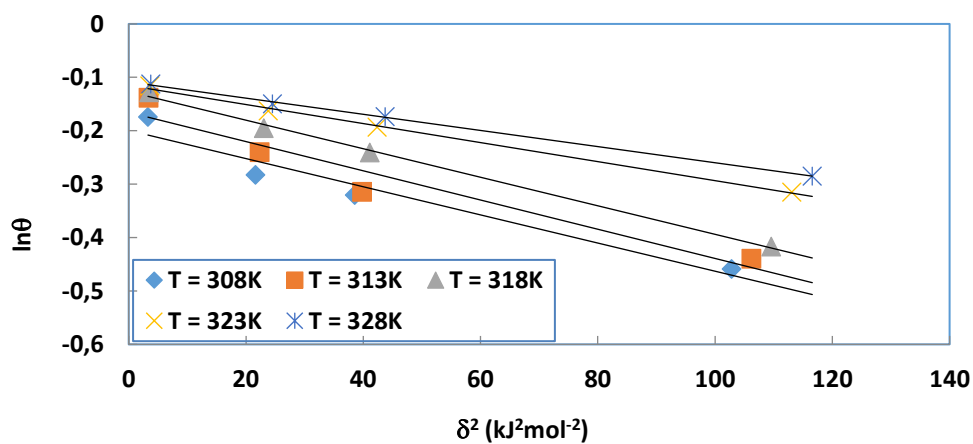


Figure 6. Dubinin-Radushkevich adsorption model for the adsorption of caffeine on copper in 1M HNO<sub>3</sub>.

Table 4. Regression parameters of Dubinin-Radushkevich isotherm

T(K)	$R^2$	$a$ (kJ <sup>-2</sup> mol <sup>2</sup> )	$E_m$ (kJ mol <sup>-1</sup> )
308	0.943	0.0026	13.87
313	0.930	0.0023	14.74
318	0.997	0.0020	15.81
323	0.997	0.0018	16.67
328	0.999	0.0015	18.26

The value of the constant  $a$  which is obtained from the slope of a straight line (see Figure 6) gives the mean adsorption energy,  $E_m$  which is the transfer energy of 1 mol of adsorbate from infinity (bulk solution) to the surface of the adsorbent.  $E_m$  is defined as:

$$E_m = \frac{1}{\sqrt{2a}} \quad (8)$$

The magnitude of  $E_m$  gives information about the type of adsorption. Values of  $E_m$  less than  $8 \text{ kJ mol}^{-1}$  [44] indicate physical adsorption. The values obtained in our work (see table 4) confirm the chemisorption process for all the range of temperatures.

### 3.3 Effect of temperature and activation parameters of the corrosion process

The effect of the temperature on the corrosion process can be evaluated using the Arrhenius equation below:

$$W = A \exp\left(-\frac{E_a}{RT}\right) \quad (9)$$

This equation can also be expressed in the logarithm form as:

$$\log W = \log A - \frac{E_a}{2.303 RT} \quad (10)$$

Where  $W$  is the corrosion rate,  $E_a$  is the apparent activation energy,  $R$  is the perfect gas constant,  $T$  is the absolute temperature and  $A$  is the frequency factor.

From the Arrhenius plots, one can obtain the values of the activation energies using the slopes of the regression lines. All the obtained values are listed in table 5.

The effect of the temperature on the corrosion process can also be investigated by determining the change in activation enthalpy  $\Delta H_a^*$  and the change in activation entropy  $\Delta S_a^*$  using the transition state equation:

$$W = \left(\frac{RT}{\pi h}\right) \exp\left(\frac{\Delta S_a^*}{R}\right) \exp\left(\frac{-\Delta H_a^*}{RT}\right) \quad (11)$$

This equation can be expressed as:

$$\log\left(\frac{W}{T}\right) = \left[\log\left(\frac{R}{\pi h}\right) + \left(\frac{\Delta S_a^*}{2.303R}\right)\right] - \frac{\Delta H_a^*}{2.303RT} \quad (12)$$

Where  $\Delta S_a^*$  is change in apparent activation entropy,  $\Delta H_a^*$  is change in apparent activation enthalpy,  $R$  is the perfect gas constant,  $\pi$  is the Avogadro number and  $h$  is the Planck's constant.

The plots of  $\log W$  against  $1/T$  for copper in 1M  $\text{HNO}_3$  in the absence and presence of different concentrations of caffeine are shown in Figure 7. The transition state plots of  $\log\left(\frac{W}{T}\right)$  versus  $(1/T)$  is given in Figure 8.

The transition plots were used to determined  $\Delta S_a^*$  and  $\Delta H_a^*$  from respectively the intercepts  $\left[\log\left(\frac{R}{\pi h}\right) + \left(\frac{\Delta S_a^*}{2.303R}\right)\right]$  and the slopes  $\left(-\frac{\Delta H_a^*}{2.303R}\right)$ . The obtained values are recorded in Table 5.

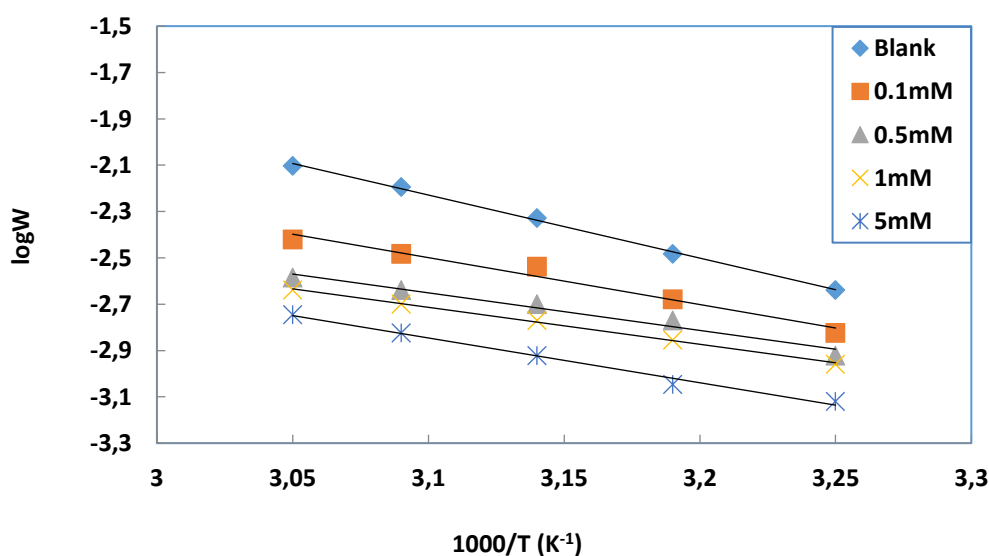


**Figure 7.** Arrhenius plots for copper corrosion in 1M  $\text{HNO}_3$  in the absence and presence of different concentrations of caffeine.



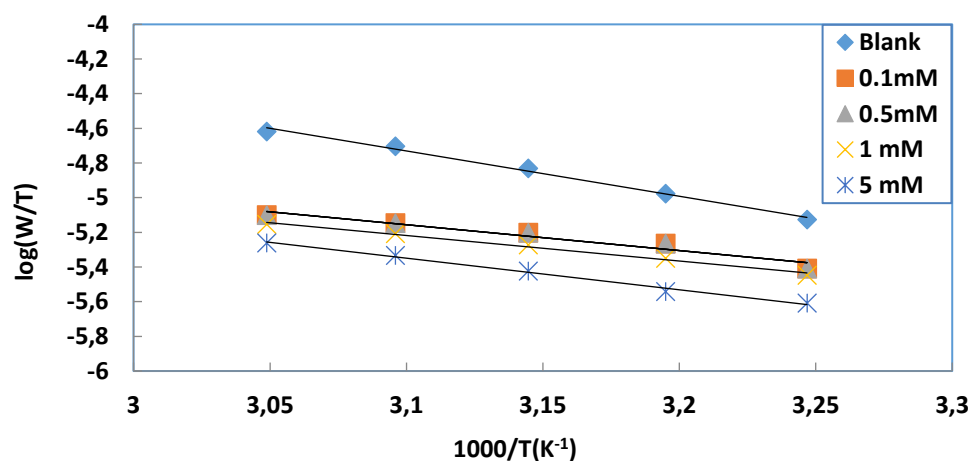


**Figure 8.** Transition state plots at different concentrations of caffeine.

**Table 5.** Thermodynamic activation parameters of the dissolution of copper in 1 M HNO<sub>3</sub> in absence and presence of caffeine.

$C_{inh}$ (mM)	$E_a$ (kJ mol <sup>-1</sup> )	$\Delta H_a^*$ (kJ mol <sup>-1</sup> )	$\Delta S_a^*$ (J mol <sup>-1</sup> K <sup>-1</sup> )
0	52.05	49.94	-132.8
0.1	38.70	28.49	-207.8
0.5	31.01	28.45	-207.6
1	30.50	28.34	-209.7
5	36.95	34.85	-191.4

According to [45], the higher value of apparent activation energy of corrosion process in the presence of an inhibitor when compared to that in its absence is attributed to its physical adsorption, its chemisorptions is pronounced in the opposite case. In our work  $E_a$  of inhibited solutions are lower than that of the uninhibited solution (blank) indicating a chemisorption mode of adsorption. The positive sign of  $\Delta H_a^*$  reflects an endothermic dissolution process leading to a slow dissolution of copper in the medium.  $\Delta S_a^*$  has a negative sign, showing that disorder decreases on going from reactant to activated complex.

### 3.4 Quantum chemical studies

The optimized structure of Caffeine is presented in Figure 9.

The values of the calculated quantum chemical parameters are listed in table 6.  $E_{HOMO}$  [46] is often associated with the electron donating ability of a molecule. An increase in the values of  $E_{HOMO}$  can facilitate the adsorption and therefore the inhibition efficiency, by indicating the disposition of the molecule to donate electrons to an appropriate acceptor with empty molecular orbital. The LUMO energy on the other hand [46], indicates the ability of the molecule to accept electrons. The lower the value of  $E_{LUMO}$ , the more probable it is that the molecule accepts electrons. In the same way, low values of the energy gap  $\Delta E = E_{LUMO} - E_{HOMO}$  lead to good inhibition efficiencies because [47] the energy to remove an electron from the last occupied orbital will be low. High values of the dipole moment  $\mu$  [48] will favor the accumulation of the inhibitor molecules on the metallic surface.

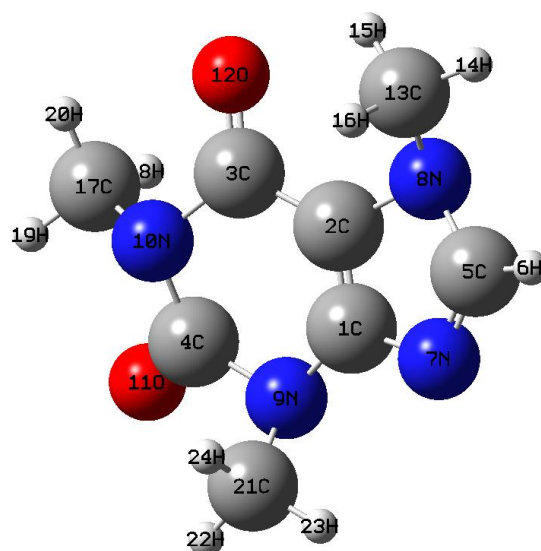


**Figure 9.** Optimized structure of caffeine (DFT/6-31+G (d)).

**Table 6.** Quantum chemical descriptors for caffeine obtained with DFT at B3LYP/6-31+G (d) and B3LYP/LanL2DZ.

Quantum descriptor	B3LYP/6-31+G(d)	B3LYP/LanL2DZ
$E_{\text{LUMO}}$ (eV)	-1.251	-1.437
$E_{\text{HOMO}}$ (eV)	-6.304	-6.367
$\Delta E$ (eV)	5.053	4.930
Dipole moment $\mu$ (Debye)	4.071	4.154
Ionization energy $I$ (eV)	6.304	6.367
Electronic affinity $A$ (eV)	1.251	1.437
Electronegativity $\chi$ (eV)	3.777	3.902
Global hardness $\eta$ (eV)	2.526	2.465
Global softness $S$ (eV <sup>-1</sup> )	0.396	0.406
Fraction of electrons transferred $\Delta N$	0.238	0.219

On the other hand, survey of literature [49, 50] reveals that several irregularities appeared in case of correlation of dipole moment with inhibition efficiency.

The basic relationship of the density functional theory of chemical reactivity [51] is the one that links the chemical potential  $\mu_P$  of DFT with the first

derivative of  $E$  with respect to the number of electrons, and therefore with the negative of the electronegativity  $\chi$ :

$$\mu_P = \left( \frac{\partial E}{\partial N} \right)_{v(r)} = -\chi \quad (13)$$

Where  $\mu_P$  is the chemical potential,  $E$  is the total energy,  $N$  is the number of electrons and  $v(r)$  is

the external potential of the system.

Hardness ( $\eta$ ) [52] has been defined within the DFT as the second derivative of  $E$  with respect to  $N$  at  $v(r)$  as a property which measures both the stability and reactivity of the molecule:

$$\eta = \left( \frac{\partial^2 E}{\partial N^2} \right)_{v(r)} \quad (14)$$

From the values of the total electronic energy, the ionization potential ( $I$ ) and the electron affinity ( $A$ ) of the inhibitors are calculated using the following equations:

$$I = E_{(N-1)} - E_N \quad (15)$$

$$A = E_{(N)} - E_{(N+1)} \quad (16)$$

$\chi$  and  $\eta$  can be written in function of  $I$  and  $A$  as:

$$\chi = \frac{I+A}{2} \quad (17)$$

$$\eta = \frac{I-A}{2} \quad (18)$$

The global softness ( $S$ ) [52] is the inverse of the global hardness:

$$S = \frac{1}{\eta} \quad (19)$$

Electronegativity, hardness and softness have proved to be very useful quantities in chemical reactivity theory. When two systems, metal and inhibitor, are brought together, electrons will flow from lower  $\chi$  (inhibitor) to higher  $\chi$  (metal), until the chemical potentials become equal. The number of transferred electrons ( $\Delta N$ ) was calculated using the equation below:

$$\Delta N = \frac{\chi_{Cu} - \chi_{inh}}{2(\eta_{Cu} + \eta_{inh})} \quad (20)$$

Where  $\chi_{Cu}$  and  $\chi_{inh}$  denote respectively the absolute electronegativity of copper and the inhibitor,  $\eta_{Cu}$  and  $\eta_{inh}$  are respectively the global hardness of copper and the inhibitor. In this work  $\Delta N$  has been determined using  $\chi_{Cu} = 4.98 \text{ eV}$  [53] and  $\eta_{Cu} = 0$  [54], assuming that for a metallic bulk  $I = A$  because they are softer than the neutral metallic atoms.

The results obtained (see Table 6) show that the high inhibition efficiency value of caffeine can be explained by its high value of  $E_{HOMO}$  (-6.314 and -6.367 eV respectively for B3LYP/6-31G (d) and B3LYP/LanL2DZ) when considering the values reported in the literature [55-57]. This high value indicates the tendency to donate electrons to empty molecular orbital of copper ions ( $Cu^{2+}$ :  $[Ar]3d^9$ ). The

low value of  $E_{LUMO}$  (-1.251 or -1.437 eV respectively with B3LYP/6-31G (d) or B3LYP/LanL2DZ) compared to that reported in the literature [55, 58] indicates its ability to accept electrons. Consequently, the HOMO-LUMO energy gap provides a measure of the stability of the formed complex on the metal surface. For the case of the dipole moment  $\mu$ , the obtained value (4.071 or 4.154 respectively for B3LYP/6-31G (d) or B3LYP/LanL2DZ) is high implying its effectiveness as a corrosion inhibitor. Similar results [59] have been reported.

The use of Mulliken population analysis to probe the adsorption centers of inhibitors have been widely reported [60-64]. There is a general consensus by several authors that the more negatively charged an heteroatom is the more it can be adsorbed on the metal surface through donor-acceptor type reaction [65-68]. It has also been reported that electrophiles attack molecules at sites of negatives charge [69], which means that sites of ionic reactivity can be estimated from atomic charges in a molecule. Mulliken populations [70] are extremely basis sets dependent that is why we have chosen to express the charges in the most used basis set (B3LYP/6-31G (d)). Thus from the values of Mulliken charges in Table 7 and Figure 10, it is possible to observe that except C(1), C(13), C(17) and C(21), all the heteroatoms N and O in the molecule present considerable excess of negative charges. The corrosion inhibition action of the molecule can be achieved via these adsorption centers.

Local reactivity was analyzed by means of the Fukui indices to assess the active regions in terms of nucleophilic and electrophilic behavior. The site-selectivity of a chemical system is generally studied using appropriate local descriptors as local softness  $s(r)$  which is given by [71]:

$$s(r) = \left( \frac{\partial \rho(r)}{\partial \mu} \right)_{v(r)} \quad (21)$$

Such that:

$$\int s(r) dr = S \quad (22)$$

Using the definition of global softness, we can write:

$$s(r) = \left( \frac{\partial \rho(r)}{\partial N} \right)_{v(r)} \left( \frac{\partial N}{\partial \mu} \right)_{v(r)} \quad (23)$$

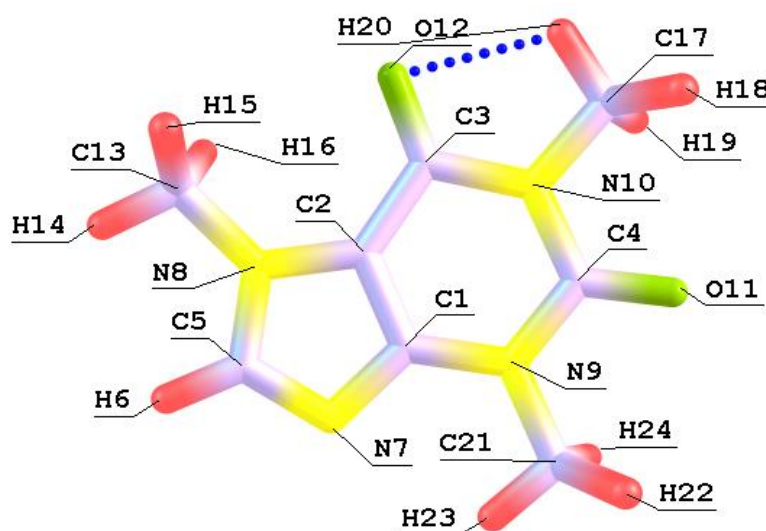
$$s(r) = f(r)S \quad (24)$$

Where  $f(r)$  [71] is defined as Fukui function:

$$f(r) = \left( \frac{\partial \rho(r)}{\partial N} \right)_{v(r)} = \left( \frac{\partial \mu}{\partial v(r)} \right)_N \quad (25)$$

**Table 7.** Fukui and local softness indices for nucleophilic and electrophilic attacks on some Caffeine atoms.

Atom N <sup>0</sup>	$q_k(N)$	$f_k^-$	$f_k^+$	$s_k^-$	$s_k^+$
C(1)	-0.755724	-0.343650	0.465217	-0.136085	0.184226
N(7)	-0.353807	-0.147656	-0.016985	-0.058472	-0.006730
N(8)	-0.333610	-0.085697	0.073580	-0.033936	0.029138
N(9)	-0.332960	-0.176659	0.069624	-0.069957	0.027571
N(10)	-0.396238	-0.175471	0.113012	-0.069486	0.044753
O(11)	-0.510311	-0.190458	0.007796	-0.075421	0.003087
O(12)	-0.566210	-0.183982	-0.051514	-0.072857	-0.020399
C(13)	-0.447747	0.058257	-0.071379	0.023070	0.028266
C(17)	-0.453557	0.044684	-0.011293	0.017695	-0.004468
C(21)	-0.550075	-0.082890	0.008034	-0.032824	0.003181

**Figure 10.** Molecule of Caffeine with the natures and labels of the atoms.

The second relation can be obtained using the relation that density is the first partial derivative of energy with respect to external potential at constant  $N$ . The Fukui function describes the sensitivity of chemical potential of a system to a local external potential. Using left and right derivatives with respect to the number of electrons, electrophilic and nucleophilic Fukui function and local softness can be defined. To described site selectivity or reactivity of an atom in a molecule, it is necessary to condense the values of  $f(r)$  and  $s(r)$  around each atomic site into single value that characterizes the atom in a molecule.

This can be achieved by electronic population analysis. Thus for an atom  $k$  in a molecule, depending upon the type of electron transfer, we have three different types of condensed Fukui function of the atom  $k$ .

$$f_{k^+} = [q_k(N+1) - q_k(N)] \text{ for nucleophilic attack} \quad (26)$$

$$f_{k^-} = [q_k(N) - q_k(N-1)] \text{ for electrophilic attack} \quad (27)$$

$$f_{k^0} = [q_k(N+1) - q_k(N-1)] \text{ for radical attack} \quad (28)$$

Where  $q_k(N+1)$ ,  $q_k(N)$  and  $q_k(N-1)$  are the charges of the atoms on the systems with  $N+1$ ,  $N$  and  $N-1$  electrons respectively. The preferred site for nucleophilic attack is the atom or region in the molecule where the value of  $f_{k+}$  is the highest while the site for electrophilic attack is the atom/region in the molecule where the value of  $f_{k-}$  is the highest.

$f_{k+}$  measures the changes of density when the molecule gains electrons and it corresponds to reactivity with respect to nucleophilic attack. On the other hand,  $f_{k-}$  corresponds to reactivity with respect to electrophilic attack or when the molecule loss electrons. According to Fukui indices **C (1)** is the most reactive site for nucleophilic attack and **C (13)** and **C (17)** are the preferred sites of electrophilic attack.

#### 4. CONCLUSION

Caffeine was found to be an effective inhibitor for copper in 1M  $\text{HNO}_3$  solution and its inhibition efficiency was concentration and temperature dependent. The corrosion process was inhibited by adsorption of the molecules of caffeine on copper surface following the modified Langmuir adsorption isotherm. Phenomenon of chemisorption is proposed from the values of activation energy ( $E_a$ ) and change in Gibbs Free energy. The negative value of Gibbs free energy is an indication of a spontaneous adsorption process. Quantum chemical calculations revealed that adsorption of caffeine is mainly concentrated around the heteroatoms (oxygen and nitrogen atoms) in the molecule. Fukui functions show the nucleophilic and electrophilic attacks sites in the molecule.

#### 5. ACKNOWLEDGMENTS

The authors gratefully acknowledged the support of the Laboratory of physical chemistry of Felix Houphouët Boigny university of Abidjan and the National Laboratory of physical health (Côte d'Ivoire).

#### 6. REFERENCES AND NOTES

- [1] Nunéz, L.; Reguera, E.; Corvo F.; Gonzalez C. *Corros. Sci.* **2005**, 47, 461. [\[CrossRef\]](#)
- [2] Tsai, H. Y.; Sun, S. C.; Wang, S. J. J. *Electrochem. Soc.* **2000**, 147, 2766. [\[CrossRef\]](#)
- [3] Ho, C. E.; Chen, W. T.; Kao, C. R. J. *Electron. Mater.* **2001**, 30, 379. [\[CrossRef\]](#)
- [4] Fiala, A.; Chibani, A.; Darchen, A.; Boulkamh, A.; Djebbar, K. *Applied Surface Science* **2007**, 253, 9347. [\[CrossRef\]](#)
- [5] Thomas, R. R.; Brusic, V. A.; Rush, B. M. J. *Electrochem. Soc.* **1992**, 139, 678. [\[CrossRef\]](#)
- [6] Chadwick, D.; Hashemi T. *Corros. Sci.* **1978**, 18, 39. [\[CrossRef\]](#)
- [7] El-Rahman H. A. A. *Corrosion* **1991**, 47, 424. [\[CrossRef\]](#)
- [8] El-Naggar M. M. J. *Mater. Sci.* **2000**, 35, 6189. [\[CrossRef\]](#)
- [9] Abd-El-Nabey, B. A.; Khamis, E.; Ramadan, M. Sh.; El-Gindy A. *Corrosion* **1996**, 52, 671.
- [10] Quraishi M. A.; Jamal, D. *Corrosion* **2000**, 56, 156. [\[CrossRef\]](#)
- [11] Lagrenée, M.; Memari, B.; Chaibi, N.; Traisnel, M.; Vezin, H.; Bentiss, F. *Corros. Sci.* **2001**, 43, 951. [\[CrossRef\]](#)
- [12] Abd-El-Rehim, S. S.; Ibrahim, M.; Khaled, K. F. J. *Appl. Electrochem.* **1999**, 29, 593. [\[CrossRef\]](#)
- [13] Bentiss, F.; Traisnel, M.; Gengembre, L.; Lagrene'e, M. *Appl. Surf. Sci.* **1999**, 152, 237. [\[CrossRef\]](#)
- [14] Hosseini, M. G.; Mertens, S. F. L.; Ghorbani, M.; Arshadi, M. R. *Mater. Chem. Phys.* **2003**, 78, 800. [\[CrossRef\]](#)
- [15] Migahed, M.; Mohamed, H. M.; Al-Sabagh, A. M. *Mater. Chem. Phys.* **2003**, 80, 169. [\[CrossRef\]](#)
- [16] Khamis, E.; El-Ashry, E. S. H.; Ibrahim, A. K. *Br Corros. J.* **2000**, 35, 150. [\[CrossRef\]](#)
- [17] Quraishi, M.; Sharma, H. K. *Mater. Chem. Phys.* **2002**, 78, 18. [\[CrossRef\]](#)
- [18] Popova, A.; Sokolova, E.; Raicheva, S.; Christov M. *Corros. Sci.* **2003**, 45, 33. [\[CrossRef\]](#)
- [19] Quraishi M. A.; Rawat J. *Mater. Chem. Phys.* **2002**, 77, 43. [\[CrossRef\]](#)
- [20] El-Azhar M.; Menari, B.; Traisnel, M.; Bentiss, F.; Lagrene'e, M. *Corros. Sci.* **2001**, 43, 2229. [\[CrossRef\]](#)
- [21] Stupnisek-lisac, E.; Bozic, A. L.; Cafuk, I. *Corrosion* **2008**, 54, 73.
- [22] Abiola, O. K.; Jamesb, A. O. *Corros. Sci.* **2010**, 52, 661. [\[CrossRef\]](#)
- [23] Solomon, M. M.; Umoren, S. A.; Udosoro, I. I.; Udoh A. P. *Corros. Sci.* **2010**, 52, 2848. [\[CrossRef\]](#)
- [24] Satapathi, A. K.; Gunasekaran, G.; Kumar, A.; Rodrigues, P. V. *Corros. Sci.* **2009**, 51, 1317.
- [25] Khaled, K. F. *Int. J. Electrochem. Sci.* **2008**, 3, 462.
- [26] Mu, G.; Li, X. J. *Colloid Interface Sci.* **2005**, 289, 184. [\[CrossRef\]](#)
- [27] Obot, I. B.; Obi-Egbedi, N. O. *Colloids and Surfaces A: Physicochem. Eng. Aspects* **2008**, 330, 207. [\[CrossRef\]](#)
- [28] Obot I. B.; Obi-Egbedi, N. O. *Surf. Rev. Lett.* **2008**, 15, 903. [\[CrossRef\]](#)
- [29] Obot, I. B.; Obi-Egbedi, N. O.; Umoren S. A. *Corros. Sci.* **2009**, 51, 276. [\[CrossRef\]](#)
- [30] Pearson, R. G. *J. Am. Chem. Soc.* **1963**, 85, 3533. [\[CrossRef\]](#)
- [31] Zarrouk, A.; Hammouti, B.; Touzani, R.; Al-Deyab, S. S.; Zertoubi, M.; Dafali, A.; Elkadiri, S. *Int. J. Electrochem. Sci.* **2011**, 6, 4939.
- [32] Becke, A. D. *J. Chem. Phys.* **1992**, 96, 9489. [\[CrossRef\]](#)
- [33] Becke, A. D. *J. Chem. Phys.* **1993**, 98, 1372. [\[CrossRef\]](#)
- [34] Frisch, M. J.; Trucks, G. W.; Schlegel, H. B.; Scuseria, G. E.; Robb, M. A.; Cheeseman, J. R.; Montgomery, J. A., Jr.; Vreven, T.; Kudin, K. N.; Burant, J. C.; Millam, J. M.;

- Iyengar, S. S.; Tomasi, J.; Barone, V.; Mennucci, B.; Cossi, M.; Scalmani, G.; Rega, N.; Petersson, G. A.; Nakatsuji, H.; Hada, M.; Ehara, M.; Toyota, K.; Fukuda, R.; Hasegawa, J.; Ishida, M.; Nakajima, T.; Honda, Y.; Kitao, O.; Nakai, H.; Klene, M.; Li, X.; Knox, J. E.; Hratchian, H. P.; Cross, J. B.; Adamo, C.; Jaramillo, J.; Gomperts, R.; Stratmann, R. E.; Yazyev, O.; Austin, A. J.; Cammi, R.; Pomelli, C.; Ochterski, J. W.; Ayala, P. Y.; Morokuma, K.; Voth, G. A.; Salvador, P.; Dannenberg, J. J.; Zakrzewski, V. G.; Dapprich, S.; Daniels, A. D.; Strain, M. C.; Farkas, O.; Malick, D. K.; Rabuck, A. D.; Raghavachari, K.; Foresman, J. B.; Ortiz, J. V.; Cui, Q.; Baboul, A. G.; Clifford, S.; Cioslowski, J.; Stefanov, B. B.; Liu, G.; Liashenko, A.; Piskorz, P.; Komaromi, Martin, I.; R. L.; Fox, D. J.; Keith, T.; Al-Laham, M. A.; Peng, C. Y.; Nanayakkara, A.; Challacombe, M.; Gill, P. M. W.; Johnson, B.; Chen, W.; Wong, M. W.; Gonzalez, C.; Pople, J. A. *Gaussian 03, Revision B.05, Gaussian, Inc., Pittsburgh PA, 2003*.
- [35] Moretti, G.; Quartarone, G.; Tassan, A.; Zingales, A. *Werkst. U. Korros.* **1999**, 45, 641. [\[CrossRef\]](#)
- [36] Villamil, R. F. V.; Corio, P.; Rubin, J. C.; Agostinho, S. M. I. *J. Electroanal. Chem.* **1999**, 472, 112. [\[CrossRef\]](#)
- [37] Vashi, R. T.; Champaneri, V. A. *Ind. J. Chem. Tech.*, **1997**, 4, 180.
- [38] Fils, J.; Zakrocinski, T.; *J. Electrochem. Soc.* **1996**, 143, 2458. [\[CrossRef\]](#)
- [39] Eduok, E. E.; Umoren, S. A.; Udoh, A. P. *Arab. J. Chem.* **2012**, 5, 334. [\[CrossRef\]](#)
- [40] Abboud, Y.; Hammouti, B.; Abourriche, A.; Bennamara, A.; Hannache H. *Res. Chem. Intermed.* **2012**, 38, 1600. [\[CrossRef\]](#)
- [41] Nazeer, A. A.; El-Abassy, H. M.; Fouda, A. S. *J. Mater. Eng. Perform.* **2013**, 22, 6321.
- [42] Gemeay, A. H.; El-Sherbiny, A. S.; Zaki, A. B. *J. Colloid Interface Sci.* **2002**, 245, 116. [\[CrossRef\]](#)
- [43] Mall, I. D.; Srivastava, V. C.; Agarwal, N. K.; Mishra, I. M. *Colloids Surf. A: Physicochem. Eng. Asp.* **2005**, 264, 17. [\[CrossRef\]](#)
- [44] Noor, E. A. *J. Appl. Electrochem.* **2009**, 39, 1465. [\[CrossRef\]](#)
- [45] Umoren, S. A.; Obot, I. B.; Apkario, L. E. *Pigm. Resin Technol.* **2008**, 37, 98. [\[CrossRef\]](#)
- [46] Popova, A.; Christov, M.; Deligeorgiev, T. *Corrosion* **2003**, 59, 756. [\[CrossRef\]](#)
- [47] Khaled, K. F. *Electrochim. Acta* **2003**, 48, 2493. [\[CrossRef\]](#)
- [48] Quraishi, M. A.; Sardar, R. *J. Appl. Electrochem.* **2003**, 33, 1163. [\[CrossRef\]](#)
- [49] Khaled, K. F.; Babic-Samardzija, N. K.; Hackerman, N. *Electrochim. Acta* **2005**, 50, 2515. [\[CrossRef\]](#)
- [50] Bereket, G.; Hur, E.; Ogretir, C. *J. Mol. Struct. (Theochem.)* **2002**, 578, 79. [\[CrossRef\]](#)
- [51] Parr, R. G.; Donnelly, R. A.; Levy, M.; Palke, W. E. *J. Chem. Phys.* **1978**, 68, 3801. [\[CrossRef\]](#)
- [52] Parr, R. G.; Pearson, R. G. *J. Am. Chem. Soc.* **1983**, 105, 7512. [\[CrossRef\]](#)
- [53] Michaelson, H. B. *Journal of Applied Physics*, **1977**, 48, 4729. [\[CrossRef\]](#)
- [54] Dewar M. J. S.; Zebisch E. G.; Healy E. F.; Stewart J. P. *J. Am. Chem. Soc.* **1985**, 107, 3902. [\[CrossRef\]](#)
- [55] Yadav, D. K.; Maiti, B.; Quraishi, M. A. *Corrosion Science* **2010**, 52, 3586. [\[CrossRef\]](#)
- [56] Obot, I. B.; Obi-Egbedi, N. O.; Umoren, S. A. *Corrosion Science* **2009**, 51, 276. [\[CrossRef\]](#)
- [57] Bentiss, F.; Lebrini, M.; Lagrenée, M.; Traisnel, M.; Elfarouk, A.; Vezin, N. *Electrochim. Acta* **2007**, 52, 6865. [\[CrossRef\]](#)
- [58] Zarrouk, A.; Hammouti, B.; Zarrok, H.; Warad, I.; Bouachrine, M. *Der Pharma Chemica*, **2011**, 3, 263.
- [59] Sahin, M.; Gece, G.; Karci, F.; Bilgic, S. *J. Appl. Electrochim.* **2008**, 38, 809. [\[CrossRef\]](#)
- [60] Assaf, F. H.; Abou-Krish, M.; El-Shahawy, A. S.; Makhoul, M.; Soudy, H. *Int. J. Electrochem. Sci.* **2007**, 2, 169.
- [61] Fang, J.; Li, J. *J. Mol. Struct. (THEOCHEM)* **2002**, 593, 179. [\[CrossRef\]](#)
- [62] Hasanov, R.; Sadikoglu, M.; Bilgic, S. *Appl. Surf. Sci.* **2007**, 253, 3913. [\[CrossRef\]](#)
- [63] Allam, N. K. *Appl. Surf. Sci.* **2007**, 253, 4570. [\[CrossRef\]](#)
- [64] Kandemirli, F.; Sagdina, S. *Corros. Sci.* **2007**, 49, 2118. [\[CrossRef\]](#)
- [65] Bereket, G.; Ogretic, C.; Ozsahim, C. *J. Mol. Struct. (THEOCHEM)* **2003**, 663, 39. [\[CrossRef\]](#)
- [66] Ozcan, M.; Dehri, I.; Erbil, M. *Appl. Surf. Sci.* **2004**, 236, 155. [\[CrossRef\]](#)
- [67] Li, W.; He, Q.; Pei, C.; Hou, B. *Electrochim. Acta* **2007**, 52, 6386. [\[CrossRef\]](#)
- [68] Wang, D.; Li, S.; Ying, Y.; Wang, M.; Xiao, H.; Chen, Z. *Corros. Sci.* **1999**, 41, 1911. [\[CrossRef\]](#)
- [69] Ozcan, M.; Dehri, I. *Prog. Org. Coat.* **2004**, 51, 181. [\[CrossRef\]](#)
- [70] Foresman J., Frisch A., *Gaussian Inc.* **1996**, 194.
- [71] Parr, R. G.; Yang, W. *J. Am. Chem. Soc.* **1984**, 106, 4049. [\[CrossRef\]](#)